Statistical Analysis of Instantaneous Frequency Scaling Factor as Derived from Optical Disdrometer Measurements at V/W Bands

Michael Zemba[1], James Nessel[1], Nicholas Tarasenko[2], Steven Lane[2]
[1] Advanced High Frequency Branch, NASA Glenn Research Center, Cleveland, OH, USA
[2] Space Vehicles Directorate, Air Force Research Laboratory, Kirtland AFB, Albuquerque, NM, USA

***Abstract*— Since October 2015, NASA Glenn Research Center (GRC) and the Air Force Research Laboratory (AFRL) have collaboratively operated an RF terrestrial link in Albuquerque, New Mexico to characterize atmospheric propagation phenomena at 72 and 84 GHz. The W/V-band Terrestrial Link Experiment (WTLE) consists of coherent transmitters at each frequency on the crest of the Sandia Mountains and a corresponding pair of receivers in south Albuquerque. The beacon receivers provide a direct measurement of the link attenuation, while concurrent weather instrumentation provides a measurement of the atmospheric conditions.**

Among the available weather instruments is an optical disdrometer which yields an optical measurement of rain rate, as well as droplet size and velocity distributions (DSD, DVD). In particular, the DSD can be used to derive an instantaneous scaling factor (ISF) by which the measured data at one frequency can be scaled to another – for example, scaling the 72 GHz to an expected 84 GHz timeseries. Given the availability of both the DSD prediction and the directly observed 84 GHz attenuation, WTLE is thus uniquely able assess DSD-derived instantaneous frequency scaling at the V/W-bands.

Previous work along these lines has investigated the DSD-derived ISF at Ka and Q-band (20 GHz to 40 GHz) using a satellite beacon receiver experiment in Milan, Italy [1-3]. This work will expand the investigation to terrestrial links in the V/W-bands, where the frequency scaling factor is lower and where the link is also much more sensitive to attenuation by rain, clouds, and other atmospheric effects.

***Index Terms*—drop size distribution, frequency scaling, propagation losses, radiowave propagation.**

I. Introduction

While NASA's communications architectures are currently moving toward Ka-band and optical frequencies, the agency is also investigating available spectrum in the Q/V/W-bands as a potential downlink option for its next generation relays [4]. Toward this end, NASA Glenn Research Center (GRC) and the Air Force Research Laboratory (AFRL) have initiated a joint terrestrial propagation campaign in Albuquerque, New Mexico to characterize effects of the atmosphere in the V and W-bands (72 GHz and 84 GHz) including rain and cloud attenuation, depolarization, scintillation, and gaseous absorption. The W/V-Band Terrestrial Link Experiment (WTLE) consists of a transmitter on the crest of the Sandia Mountains and a receiver on the roof of a University of New Mexico research center (COSMIAC) in south Albuquerque. The slant path spans approximately 24 km, with the receiver and transmitter at elevations of 1.6 km and 3.2 km respectively, resulting in a look angle of 3.9° above the horizon. Fig. 1 shows the location of the transmitter at Sandia Crest (top left) and the receivers on the roof of the COSMIAC building (top right). The link has been operational since October 1, 2015.

Fig. 1. The location of the transmitter atop Sandia Crest (top left), the V/W-band beacon receivers (top right) and the Thies Clima optical disdrometer (bottom) in Albuquerque, New Mexico.

The V/W-band beacon receivers provide a direct measurement of the link while collocated meteorological instrumentation provides a measurement of the ground level atmospheric conditions including temperature, pressure,

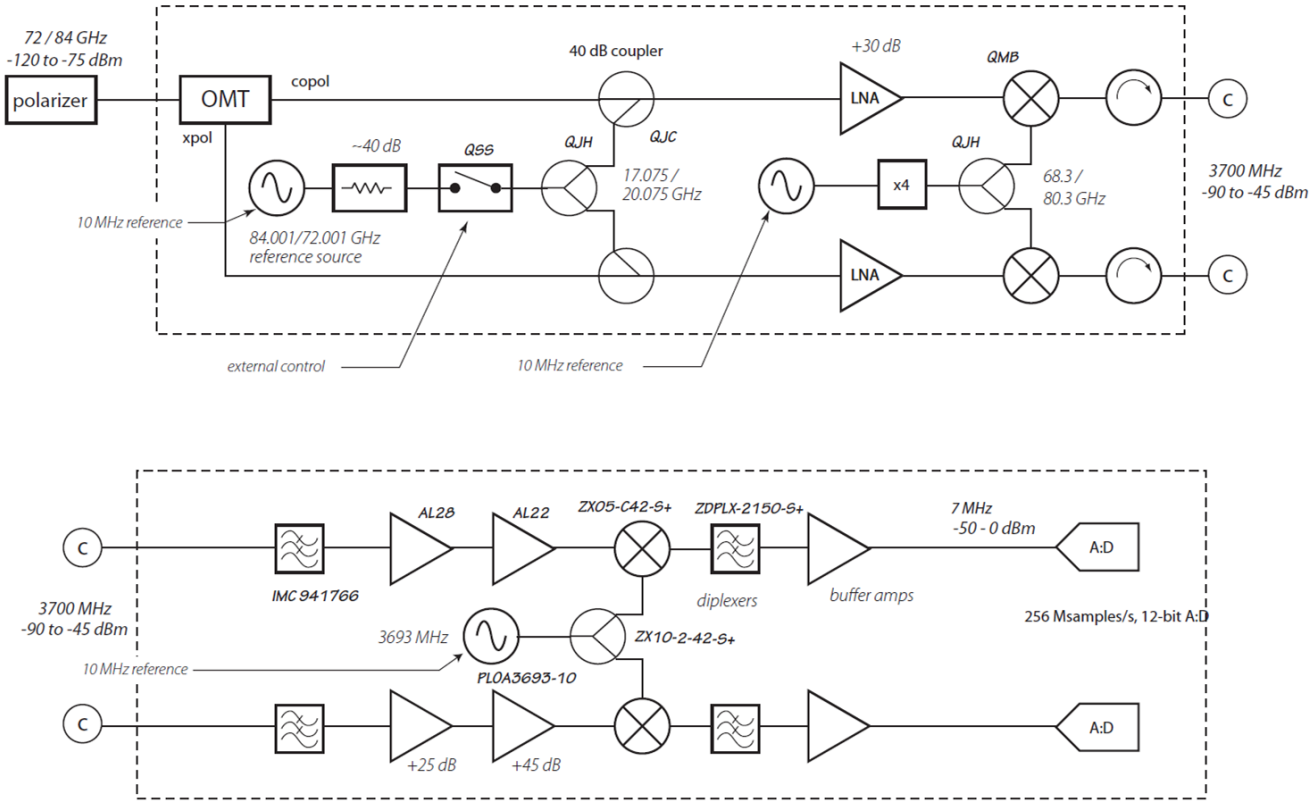

Fig. 2. Block diagram of the V/W-band beacon receiver design.

humidity, wind speed and wind direction, as well as measurements of precipitation by means of both a tipping bucket and a laser disdrometer (Fig. 1, bottom). The disdrometer yields droplet size and velocity distributions (DSD, DVD) which can be used to calculate the specific attenuation at each frequency and thereby derive a scaling factor that can translate the measured 72 GHz attenuation data to an expected 84 GHz attenuation. Given the capability of the experiment to both predict the 84 GHz attenuation from the DSD as well as measure it directly from the beacon receiver, WTLE is uniquely suited to characterize the instantaneous frequency scaling factor in terms of accuracy and statistical variation.

Previous work along these lines has investigated the DSD-derived ISF at Ka and Q-band (20 GHz and 40 GHz) using a satellite beacon receiver experiment in Milan, Italy [1-3]. This work will expand the investigation to terrestrial links in the V/W-bands, between which the frequency scaling factor is lower and where the links are also much more sensitive to attenuation by atmospheric phenomena.

II. Experiment Design

A. W/V-Band Terrestrial Link Experiment

The WTLE transmitter consists of two coherent continuous wave (CW) beacons at 72 and 84 GHz with an EIRP of 40 dBm using two lens antennas with a 3° beam-width and 35 dBi directivity. The transmitter, including the lens antennas, is contained in a weather-proof enclosure with the electronics temperature controlled to within ±0.01°C and air temperature controlled to within ±0.1°C. Polarization is LHCP from the perspective of the receivers.

The receiver system (Fig. 2) consists of two 0.5m V and W-band Cassegrain reflectors (Fig. 1, top left). The twin receivers observe both the co- and cross-polarization components of each channel and downconvert the signals to 7 MHz at the feed before digitization. The receiver electronics are also temperature controlled to within ±0.01°C, and a calibration tone is injected before the LNA for use in periodically monitoring overall system gain. All downconversion stages are referenced to a common ultra-stable 10 MHz citrine oscillator. After digitization, the signals are processed using an algorithm developed in previous NASA propagation terminals [5, 6] which uses a frequency estimation technique to coherently track and measure the amplitude of the beacon signals [7]. An overall measurement rate of 10 Hz rate is implemented in order to characterize scintillation effects. Ultimately, the receivers achieve a dynamic range of approximately 75 dB. More information on the experiment design and instrumentation is presented in [8].

B. Thies Clima Disdrometer

The Thies Clima Laser Precipitation Monitor or disdrometer, pictured in Fig. 1 (bottom), is located alongside

the beacon receivers at COSMIAC and is the same model as that used in the Ka/Q-band Milan analysis [1-3]. It operates by means of an infrared laser diode which generates a 785 nm beam over an area of 4560 mm^2. A photodiode monitors fluctuations in the received signal power as precipitating particles cross the beam. Using this information, the particle diameter and velocity are derived from the magnitude and duration of the signal attenuation. The observed particles are classified into spectra of 22 diameter bins from 0.125 mm to 8 mm and 20 velocity bins from 0 to 10 m/s [9]. Through on-board processing, the instrument also classifies the type of precipitation and intensity. Measurements are recorded in one minute intervals.

III. Data Analysis

A. Derivation of Scaling Factor

The instantaneous frequency scaling factor can be derived from the disdrometer data by using the DSD to calculate the specific attenuation (γ) at the frequencies of interest. The ratio of the two, γ_{84} / γ_{72}, is then used to scale the measured 72 GHz data to 84 GHz, which may then be compared with the measured data taken directly at 84 GHz. The calculation of specific attenuation for a given drop density distribution N(D) is a function of the wavelength λ and the forward scattering coefficient Re{S(0)} as in [10]:

$$\gamma = 4.343 \times 10^3 \frac{\lambda^2}{\pi} \sum Re\{S(0)\} N(D) \Delta D \qquad (1)$$

where ΔD is the drop size interval (in mm). For this analysis, the forward scattering coefficient is calculated using the Mie scattering model [11], which assumes a spherical droplet shape. Previous work has investigated the impact of a scattering model with a non-spherical droplet, such as the T-matrix method, and concluded that differences over the Mie model are negligible when the droplets are generally small and the polarization is not along the axis of droplet elongation (i.e. circular or linear slant) [3]. The scattering computation, as well as the calculation of the drop density distribution from the binned DSD data, are detailed in [12].

B. Analysis of Rain Events

The data used in this analysis spans from October 1, 2015 through June 30, 2016 and was first calibrated for any system gain variation using the gain calibration tone of the receiver as mentioned in Section II.A. After calibration, applicable rain events were isolated through a combination of automated and manual processing. Events were removed from the analysis if the disdrometer was not operational, if the receivers were not operational, or if rain was not measured by the disdrometer (i.e. occurring solely along the path). However, the analysis does include all other events where the disdrometer measured rain at the receiver, including those in which the receiver conditions may not be representative of conditions along the path or at the crest (as in Fig. 5, for example). This is particularly notable for the WTLE link, more so than for the

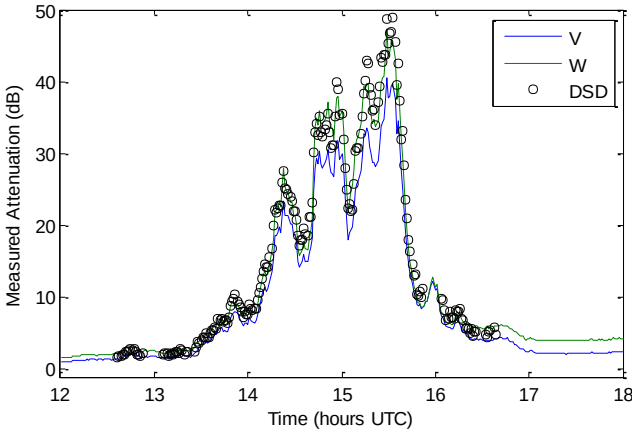

Fig. 3. Example of a light rain event (up to 4 mm/hr) on April 8th, 2016, comparing the measured rain attenuation to the predicted value calculated from the DSD. The prediction tracks well throughout the event.

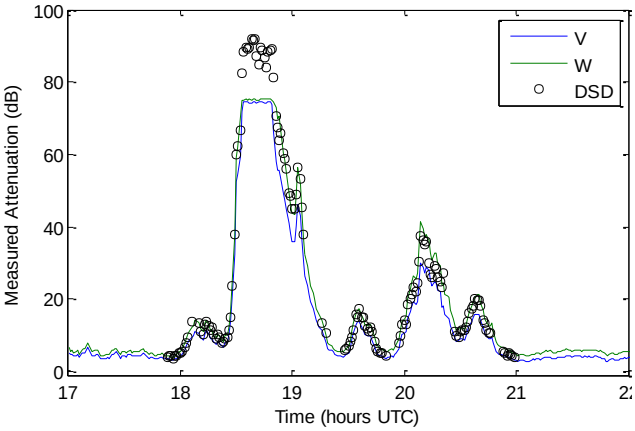

Fig. 4. Example of a heavy rain event (up to 25 mm/hr) on November 4th, 2015, comparing the measured rain attenuation to the predicted value calculated from the DSD. Attenuation exceeds the system dynamic range on both channels (75 dB) from approximately 18:30 – 18:45 UTC.

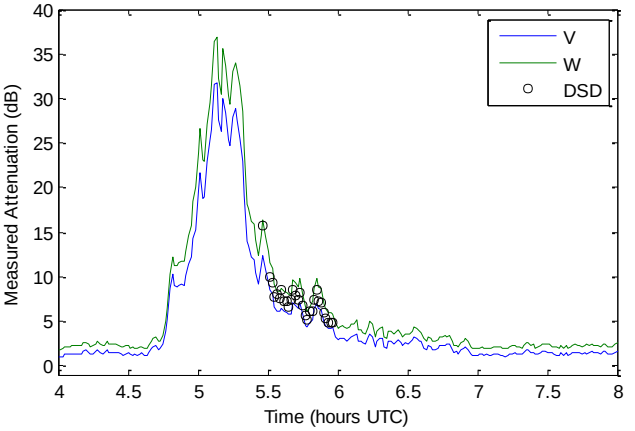

Fig. 5. Example of a light rain event (less than 0.1 mm/hr) on October 24th, 2015, comparing the measured rain attenuation to the predicted value calculated from the DSD. Attenuation up to 11.6 dB is measured during the first half of the event, but no rain is measured at the site, indicating that the rain is along the path. By the end of the event, light rain is detected over the receiver, and the DSD prediction tracks the measurement.

Milan link, as the rain cells in Albuquerque are generally smaller, the crest conditions are often unique, and the higher frequency V/W link is generally more susceptible to attenuation from atmospheric influences than the Ka/Q link.

For each rain event, the attenuation level before and after the event was averaged and subtracted from the measured rain attenuation to isolate the excess attenuation due to rain, though this method is not perfect and other sources of attenuation (e.g. clouds) may still bias the result. Instances where this was readily apparent were removed by inspection (primarily slow-varying, high attenuation consistent with snow or water on the feed/reflector). Rainy periods were defined as any 1 minute period where the disdrometer observed more than 5 precipitating particles (roughly 0.03 mm/hr depending on particle class), and days were included in the subsequent statistical analysis if they included at least 10 minutes exceeding this level of activity. Altogether, 85 hours of rain events were isolated across 86 days containing rain.

IV. Results

A. *Time Series Results*

Time series examples are presented in Figs. 3 – 5, comparing the measured attenuation at 72 GHz (blue) and 84 GHz (green) to the predicted attenuation at 84 GHz (black) calculated by scaling the 72 GHz data with the ISF calculated from the DSD. The DSD-derived attenuation is only plotted during precipitation events as isolated by the criteria in Section III.B.

In Fig. 3, a light rain event is shown spanning approximately 4 hours. For this event, the rain rate peaked at 4 mm/hr. The attenuation predicted from the DSD-derived scaling factor tracks well with the measured attenuation for the duration of the event, with a mean error of 0.23 dB and a maximum error of 3.62 dB at 15:39 UTC.

In Fig. 4, an example of a heavy rain event is shown, spanning 4 hours. Here, the rain rate reaches up to 25 mm/hr. The predicted attenuation generally tracks well with the measured attenuation, but for approximately 15 minutes shortly before 19:00 UTC, the total attenuation exceeds the dynamic range of the receivers, eventually saturating both channels at the system noise floor of 75 dB. In periods where the V-band channel is saturated, the DSD-derived prediction is also saturated, as it relies on the V-band timeseries to derive the W-band prediction. However, in cases where only the W-band measurement channel is saturated, the W-band prediction may still be valid as it is derived from a valid V-band measurement. In this case, there is a small portion of time, a total of 3 minutes, at the beginning and end of the event where the W channel is saturated but the V timeseries is still measureable. Thus, the W-band DSD prediction has an additional 3 minutes of availability over the W-band measurement for this event. Throughout the event, a mean error of 0.28 dB is observed with a maximum error of 2.89 dB (excluding the period where the dynamic range is exceeded).

In Fig. 5, another light rain event is shown, but in this case the event occurs primarily along the path or at the crest and

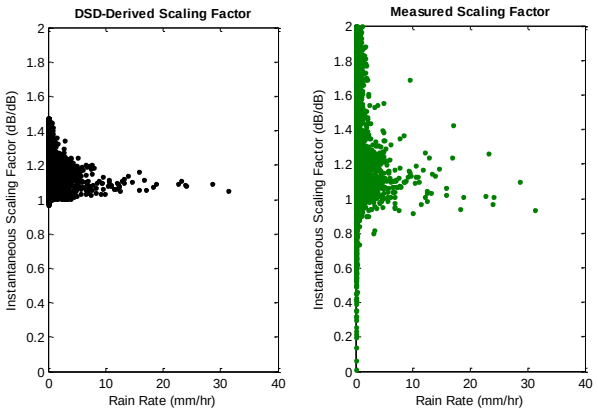

Fig. 6. The average instantaneous scaling factor for a given rain rate, as derived from the DSD (left) and as measured by the receivers (right). As shown, the scaling factor is averaged across rain rate bins of 0.05 mm/hr.

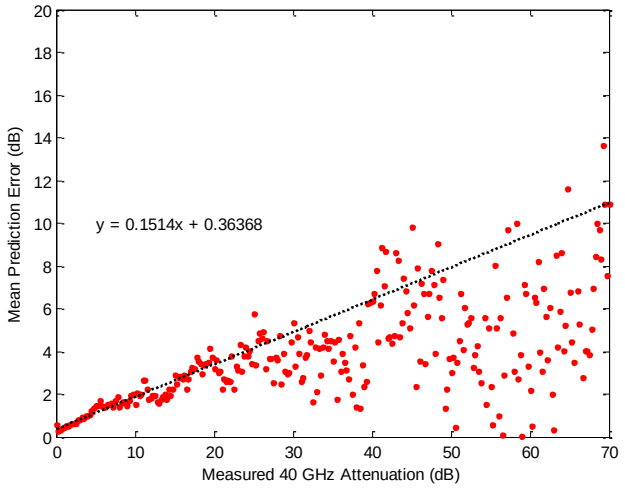

Fig. 7. The error in the DSD-predicted attenuation as a function of the measured attenuation level. A linear fit from 0 – 15 dB, where the majority of measurements are available, indicates a trend of 0.15 dB error per dB of attenuation.

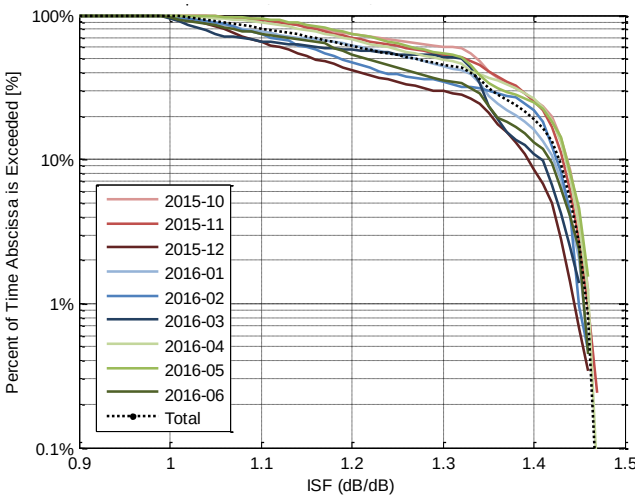

Fig. 8. The Cumulative Distribution Function (CDF) of the DSD-derived Instantaneous Scaling Factor by month as well as the total of the 9 month observation period.

precipitation is not measured by the disdrometer. About an hour and a half into the event, a small amount of rain is recorded (less than 0.1 mm / hr). As detailed in Section III.B, the first portion of this event is excluded from the statistical analysis as there is no associated disdrometer measurement, but the second portion is included as there are disdrometer measurements are available, though the measured precipitation from the disdrometer most likely does not account for the amount of loss on the link. During the measured portion of this event, the mean prediction error was much higher than the previous two examples, in which the disdrometer measurement was more representative of the link conditions. Here, the mean error was 1.11 dB with a maximum error of 1.70 dB.

B. Instantaneous Scaling Factor vs. Rain Rate

The instantaneous scaling factor is plotted against rain rate in Fig. 6, as derived from both the DSD (left) and the measured attenuation levels (right). As shown, all scaling factors observed in the 9 month observation period are averaged across rain rate bins of 0.05 mm/hr. Both the measured and DSD-derived instantaneous scaling factor tend to decrease slightly as rain rate increases, but remain very slightly above unity as expected for scaling between 72 and 84 GHz. For rain rates below 5 mm/hr, the mean instantaneous scaling factor was 1.24 dB/dB as derived from the DSD, and 1.53 dB/dB as observed from the measured attenuations.

C. Prediction Error vs. Attenuation

The error of the DSD-derived scaled attenuation as compared to the measured attenuation increases linearly as a function of attenuation level, as demonstrated in Fig. 7. All prediction error observations over the 9 month period are included and averaged across bins of 0.25 dB attenuation level. A linear fit from 0 – 20 dB indicates a trend of 0.15 dB prediction error for every 1 dB of rain attenuation. Beyond 20 dB, the noise of the prediction error increases rapidly; the ability to characterize the true prediction error deteriorates beyond this point as there are less observations at these attenuation levels.

D. Statistics of Scaling Factor

Lastly, Fig. 8 presents the cumulative distribution function (CDF) statistics of the ISF both in total and monthly. Over the 9 month period, the ISF was less than 1.43 dB/dB for 90% of observations. This did vary from month to month, but only slightly, and this is likely dependent on the amount and intensity of rain observed during a given month. The largest deviations were in December, where 90% of observations were less than 1.40 dB/dB, and in October, where 90% were less than 1.44 dB/dB.

V. CONCLUSIONS

Predictions of rain attenuation are necessary for effective design of communications systems, particularly at high frequencies, and may be derived from scaling of existing data at lower frequencies when data at the frequency of interest is not immediately available. In this work, we investigated the use of the optical disdrometer measurements to derive an instantaneous scaling factor for use in predicting rain attenuation at 84 GHz by the scaling of measured attenuation at 72 GHz. Time series examples of the scaled result were presented for different types of rain event, and various aspects of the approach were explored: the effectiveness of the DSD-derived prediction within different types of events, the trend of the instantaneous scaling factor as a function of the rain rate, and the error of the scaled attenuation prediction as a function of total attenuation level, as well as the statistics of the DSD-derived ISF. This analysis indicates that the instantaneous scaling factor decreases as a function of rain rate, but not to the extent demonstrated in previous work at lower frequencies when scaling over a larger range (20 GHz to 40 GHz) [1]. Also, the error of the scaled predicted attenuation was observed to increase linearly as a function of attenuation level -- a linear trend of 0.15 dB error per dB attenuation. Statistically, the ISF was observed to vary only slightly from month to month over the 9 month period, but a larger data set may be required for complete statistical validation.

REFERENCES

[1] J. Nessel, M. Zemba, L. Luini, C. Riva, “Comparison of Instantaneous Frequency Scaling from Rain Attenuation and Optical Disdrometer Measurements at K/Q bands”, 21st Ka and Broadband Communications Conference, Bologna, Italy, October 2015.

[2] M. Zemba, J. Nessel, J. Houts, L. Luini, C. Riva, “Statistical Analysis of Instantaneous Frequency Scaling Factor as Derived from Optical Disdrometer Measurements at K/Q Bands,”10th European Conf. on Antennas and Propag., Davos, Switzerland. April 10-15 2016.

[3] M. Zemba, L. Luini, J. Nessel, C. Riva, J. Houts, ”Impact of Scattering Model on Disdrometer Derived Attenuation Scaling,” 22nd Ka and Broadband Communications Conference, Cleveland, Ohio, October 17 – 20, 2016.

[4] Space Communications and Navigation Office, “NASA’s Space-Based Relay Study: Overview and Direction,” Washington, DC: March 2013.

[5] J. Nessel, J. Morse, M. Zemba, C. Riva, L. Luini, “Preliminary Results of the NASA Beacon Receiver for the Alphasat Aldo Paraboni TDP5 Propagation Experiment,” 20th Ka and Broadband Communications Conference, Salerno, Italy, October 2014.

[6] J. Nessel, G. Gousetis, M. Zemba, J. Houts, “Design and Preliminary Results from Edinburgh, UK Alphasat Q-band Propagation Terminal,” 22nd Ka and Broadband Communications Conference, Cleveland, Ohio, October 17 – 20, 2016.

[7] M. Zemba, J. Morse, J. Nessel, “Frequency Estimator Performance for a Software-based Beacon Receiver,” IEEE Antennas and Propagation Symposium, July 2014, pp.1574-1575.

[8] M. Zemba, J. Nessel, J. Houts, N. Tarasenko, S. Lane, D. Murrell, “Preliminary Results from the AFRL-NASA W/V-Band Terrestrial Link Experiment in Albuquerque, NM,” 2016 IEEE Int. Symp. on Antennas and Propag., Fajardo, Puerto Rico. June 26 – July 1, 2016.

[9] Thies Clima Laser Precipitation Monitor: Instructions for Use. Rev. 2.5. July 2011.

[10] M. Sadiku, Numerical Techniques in Electromagnetics, 2nd Ed., CRC Press, 2001.

[11] C. Bohren, D. Huffman, Absorption and Scattering of Light by Small Particles, Wiley, 1983.

S. Bertorelli and A. Paraboni, “Modelling of short-term frequency scaling for rain attenuation using ITALSAT data,” Int. J. Satell. Commun., vol. 25, no. 3, pp. 251–262, 2007.